FcγR responses to soluble immune complexes of varying size: A scalable cell-based reporter system

Haizhang Chen[1,2], Andrea Maul-Pavicic[3,4], Martin Holzer[5], Ulrich Salzer[3], Nina Chevalier[3], Reinhard E. Voll[3,4], Hartmut Hengel[1,2,#] & Philipp Kolb[1,2,#]

[1]Institute of Virology, University Medical Center, Albert-Ludwigs-University Freiburg, Hermann-Herder-Str. 11, 79104 Freiburg, Germany
[2]Faculty of Medicine, Albert-Ludwigs-University Freiburg, 79104 Freiburg, Germany
[3]Department of Rheumatology and Clinical Immunology, Medical Center - University of Freiburg, Faculty of Medicine, University of Freiburg, Hugstetterstr. 55, 79106 Freiburg, Germany
[4]Center for Chronic Immunodeficiency (CCI), Medical Center-University of Freiburg, Faculty of Medicine, University of Freiburg, Breisacherstr. 115, 79106 Freiburg, Germany
[5]Institute for Pharmaceutical Sciences, Albert-Ludwigs-University Freiburg, Hermann-Herder-Str. 9, 79104 Freiburg, Germany
[#]corresponding authors

Summary

This study describes a novel cell-based reporter assay enabling the detection and quantification of multimeric soluble IgG immune complexes (sICs). By selective activation of specific FcγRs, the assay shows sensitivity to sIC size and responds to synthetic and clinically relevant sICs in sera from SLE patients and autoimmune-prone mice.

Abstract

Fcγ-receptor (FcγR) activation by antibody derived soluble immune complexes (sICs) is a major contributor to inflammation in autoimmune diseases such as systemic lupus erythematosus (SLE). A robust and scalable test system allowing for the detection and quantification of sICs with regard to receptor activation is missing. We developed a comprehensive cell-based reporter system capable of measuring the sIC-mediated activation of individual human and mouse FcγRs. We show that compared to human FcγRs IIB and III, human FcγRs I and IIA lack sensitivity to sICs. Further, the assay proved to be sensitive to sIC size enabling us to demonstrate for the first time a complete translation of the Heidelberger-Kendall precipitation curve to FcγR responsiveness. The assay also proved useful to quantify sICs-mediated FcγR activation using sera from SLE patients and mouse models of lupus and arthritis. Thus, in clinical practice, it might be employed to measure FcγR activation as a biomarker for disease activity in immune-complex mediated disease.

34 **Introduction**

35 Immunoglobulin G (IgG) is the dominant immunoglobulin isotype in chronic infections and in
36 antibody-mediated autoimmune diseases. The multi-faced effects of the IgG molecule rely both
37 on the F(ab) regions, which recognize a specific antigen to form immune complexes (ICs), and
38 the constant Fc region (Fcγ), which is detected by Fcγ receptors (FcγRs) found on most cells
39 of the immune system (Lu et al., 2018). When IgG binds to its antigen ICs are formed, which,
40 depending on the respective antigen, are either cell-bound or soluble (sICs). The composition
41 of sICs is dependent on the number of epitopes recognized by IgG on a single antigen
42 molecule and the ability of the antigen to form multimers. Fcγ-FcγR binding is necessary but
43 not sufficient to activate FcγRs with receptor cross-linking generally underlying receptor
44 activation (Bruhns et al., 2009b; Ravetch and Bolland, 2001; Urlaub et al., 2019; van der Poel
45 et al., 2011). Cell bound ICs are readily able to cross-link FcγRs (Bruhns et al., 2009b; Lux et
46 al., 2013). This induces various signaling pathways (Greenberg et al., 1994; Kiefer et al., 1998;
47 Luo et al., 2010) which in turn regulate immune cell effector functions (Bournazos et al., 2017;
48 Nimmerjahn and Ravetch, 2010). It is also suggests that sICs can dynamically tune FcγR
49 activation, meaning that changes in sIC size directly impact FcγR responses (Lux et al., 2013).
50 However, the molecular requirements are largely unknown. Also, a functional reproduction of
51 the paradigmatic Heidelberger-Kendall precipitation curve, describing that the molecular size
52 of sICs determined by the antibody:antigen ratio dynamically tunes FcγR activation
53 (Heidelberger and Kendall, 1929; Heidelberger and Kendall, 1935), is missing.

54 Generally, IC-mediated FcγR cross-linking is indispensable to initiate the full signal cascade
55 following immune cell activation (Duchemin et al., 1994; Getahun and Cambier, 2015; Luo et
56 al., 2010; Urlaub et al., 2019). Human FcγRs are membrane resident receptors recognizing
57 Fcγ. Among all type I FcγRs, FcγRIIB (CD32B) is the only inhibitory one signaling via
58 immunoreceptor tyrosine-based inhibitory motifs (ITIMs) while the activating receptors are
59 associated with immunoreceptor tyrosine-based activation motifs (ITAMs). Another exception
60 is FcγRIIIB (CD16B), which is glycosylphosphatidylinositol (GPI)-anchored (Bruhns, 2012;
61 Bruhns and Jonsson, 2015; Nimmerjahn and Ravetch, 2006; Nimmerjahn and Ravetch, 2008).

62 FcγRI (CD64) is the only receptor with high affinity binding to monomeric IgG not associated
63 with antigen and is primarily tasked with phagocytosis linked to antigen processing and
64 pathogen clearance (Guilliams et al., 2014; Indik et al., 1994). All the other FcγRs only
65 efficiently bind to complexed, meaning antigen-bound IgG (Bruhns, 2012; Bruhns and
66 Jonsson, 2015; Lu et al., 2018). While FcγRI, FcγRIIB and FcγRIIIA are able to recognize sICs,
67 this has not been reported for FcγRIIA (CD32A), rather this receptor has recently been shown
68 to depend on the neonatal Fc receptor (FcRn) to do so (Fossati et al., 2002b; Hubbard et al.,
69 2020).
70 Activation of FcγRs leads to a variety of cellular effector functions such as antibody-dependent
71 cellular cytotoxicity (ADCC) by natural killer (NK) cells via FcγRIIIA, antibody-dependent
72 cellular phagocytosis (ADCP) by macrophages via FcγRI, cytokine and chemokine secretion
73 by NK cells and macrophages via FcγRIIIA. Furthermore, reactive oxygen species (ROS)
74 production of neutrophils and neutrophil extracellular traps formation (NETosis) via FcγRIIIB,
75 dendritic cell (DC) maturation and antigen presentation via FcγRIIA and B cell selection and
76 differentiation via FcγRIIB (Berger et al., 1996; Bournazos et al., 2017; Granger et al., 2019;
77 Kang et al., 2016; Laborde et al., 2007; Pincetic et al., 2014; Tay et al., 2019; Vidarsson et al.,
78 2014). Consequently, FcγRs regulate and connect both innate and adaptive branches of the
79 immune system. Various factors have been indicated to influence the IC-dependent FcγR
80 activation profiles, including Fcγ-FcγR binding affinity and avidity (Koenderman, 2019), IgG
81 subclass, glycosylation patterns and genetic polymorphisms (Bruhns et al., 2009a; Pincetic et
82 al., 2014; Plomp et al., 2017; Vidarsson et al., 2014), stoichiometric antigen-antibody-ratio
83 (Berger et al., 1996; Lux et al., 2013; Pierson et al., 2007) and FcγR clustering patterns (Patel
84 et al., 2019). For example, glycosylation patterns of the IgG Fc domain initiate either pro- or
85 anti-inflammatory effector pathways by tuning the binding affinity to activating or inhibitory
86 FcγRs, respectively (Bohm et al., 2014). However, despite being explored individually, the
87 functional consequences of these features when acting in combination on a single receptor
88 are still not fully understood. Therefore, an assay allowing for the systematic functional
89 assessment of IC-mediated FcγR activation is strongly required. sICs and immobilized ICs

90 represent intrinsically different stimuli for the immune system (Fossati et al., 2002a; Granger
91 et al., 2019). Soluble circulating ICs are commonly associated with chronic viral or bacterial
92 infections (Wang and Ravetch, 2015; Yamada et al., 2015) and some autoimmune diseases,
93 such as systemic lupus erythematosus (SLE) or rheumatoid arthritis (RA) (Antes et al., 1991;
94 Koffler et al., 1971; Zubler et al., 1976). Typically, sICs related disorders are characterized by
95 systemic cytokine secretion (Mathsson et al., 2007; Vogelpoel et al., 2015) as well as immune
96 cell exhaustion and senescence (Bano et al., 2019; Tahir et al., 2015). In order to study sIC-
97 dependent activation of FcγRs in detail, we employed a cell-based assay which has been
98 previously utilized to study immobilized ICs (Corrales-Aguilar et al., 2013) and adapted it into
99 a sIC sensitive reporter system capable of distinguishing the activation of individual FcγRs and
100 their responses to varying complex size. This allowed for the first time a complete reproduction
101 of the Heidelberger-Kendall precipitation curve measuring actual FcγR activation. The assay
102 also enables a quantification of clinically relevant sICs in sera from SLE patients and
103 autoimmune-prone mice with immune-complex-mediated arthritis and lupus using reporter
104 cells expressing chimeric mouse FcγRs.
105
106 **Results**
107
108 **Experimental assay setup**
109 The assay used in this study was adapted from a previously described cell-based FcγR
110 activation assay designed to measure receptor activation in response to opsonized virus
111 infected cells (Corrales-Aguilar et al., 2013) or therapeutic Fc-fusion proteins (Lagasse et al.,
112 2019). We changed the assay setup to enable measurement of sICs when directly incubated
113 with reporter cells stably expressing the ectodomains of the human FcγR fused to the signaling
114 module of the mouse CD3-ζ chain (FcγRI: Acc# LT744984; FcγRIIA: Acc# M28697;
115 FcγRIIB/C: Acc# LT737639; FcγRIIIA/B: Acc# LT737365). Ectodomains of FcγRIIIA and
116 FcγRIIIB as well as ectodomains of FcγRIIB and FcγRIIC are identical. Second generation
117 reporter cells were generated to stably express chimeric FcγRs compared to the stable

118 transfectants used in the original assay (Corrales-Aguilar et al., 2013). To this end, BW5147
119 cells were transduced as described previously via lentiviral transduction (Corrales-Aguilar et
120 al., 2013; Van den Hoecke et al., 2017). Human FcγR expression on transduced cells after
121 puromycin selection is shown in Fig. 1A. Activation of the reporter cells is measured by
122 quantification of mouse IL-2 (mIL-2) secretion into the cell culture supernatant using an anti-
123 IL-2 sandwich ELISA as described previously (Corrales-Aguilar et al., 2013). In order to employ
124 the original assay, designed to measure ICs on adherent infected cells, for the detection of
125 soluble ICs we first determined the suspension of IgG achieved by pre-blocking a 96 well
126 ELISA microtiter plate using PBS/10%FCS. To this end, we compared different concentrations
127 of FCS in the blocking reagent and measured the threshold at which IgG (rituximab, Rtx) no
128 longer binds to the plate and stays in solution. Fig. 1B clearly shows that FCS supplementation
129 to 1% (v/v) or higher is sufficient to keep antibodies in solution and prevents IgG binding to the
130 plastic surface. Using this adapted protocol, the assay allows for the characterization of FcγR
131 interaction with immobilized ICs versus sICs as shown schematically in Fig. 1C. Next, we set
132 out to test if immobilized IgG is an appropriate substitute for opsonized cells or immobilized
133 ICs with regard to FcγR activation as suggested before (Tanaka et al., 2009).

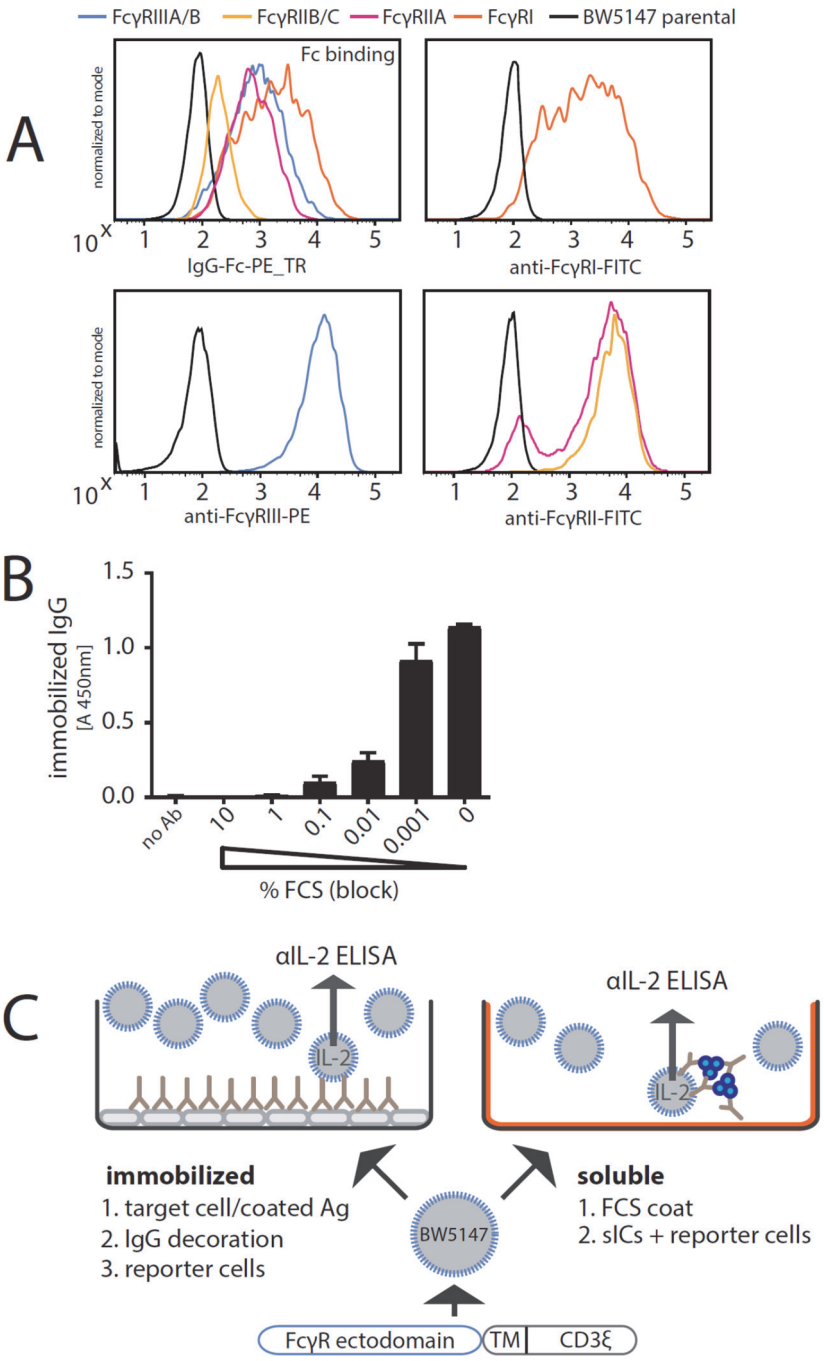

Fig. 1. Establishment of a cell-based reporter assay measuring FcγR activation in response to sICs. A) BW5147 reporter cells stably expressing human FcγRs or BW5147 parental cells were stained with FcγR specific conjugated mAbs as indicated and measured for surface expression of FcγRs via flow cytometry. Fcγ binding was determined using a PE-TexasRed-conjugated human IgG-Fc fragment. B) FCS coating of an ELISA plate allows for suspension of subsequently added IgG. Plate bound IgG was quantified via ELISA. PBS supplemented with >1% FCS (v/v) avoids adhesion of IgG (rituximab, Rtx) to the ELISA plate. C) Schematic of an immobilized IC or soluble IC setup. BW5147 reporter cells expressing chimeric human FcγR receptors secrete IL-2 in response to FcγR activation by clustered IgG. Soluble ICs are generated using mAbs and multivalent antigens (blue). Solubility is achieved by pre-blocking an ELISA plate using PBS supplemented with 10% FCS (orange).

146 There was no qualitative difference in FcγR activation between immobilized Rtx, immobilized
147 ICs (Rtx + CD20) or Rtx-opsonized 293-CD20 cells, showing that FcγR cross-linking by
148 clustered IgG alone is sufficient for receptor activation (Fig. 2). As sICs formed by monomeric
149 CD20 peptide (aa 141-188) and Rtx completely failed to activate FcγRs, we hypothesized that,
150 in order to generate sICs able to activate FcγRs, antigens have to be multivalent. Of note, to
151 reliably and accurately differentiate between soluble and immobilized triggers using this assay,
152 reagents for the generation of ICs need to be of high purity and consistent stability. Only
153 combinations of therapy grade ultra-pure mAbs and ultra-pure antigens (size exclusion
154 chromatography) showed reproducible, dose-dependent and specific activation of the reporter
155 assay (data not shown).
156

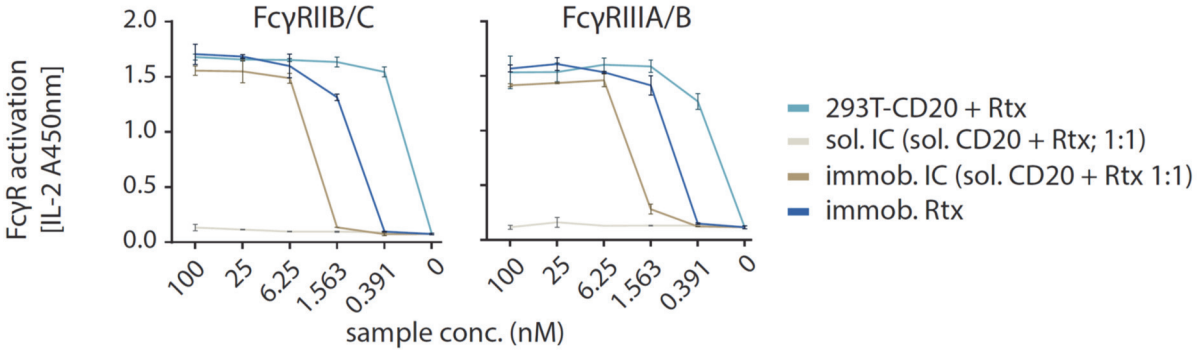

157

158 **Fig. 2. FcγRIIB/C and FcγRIIIA/B do not respond to small hetero-dimeric sICs but are**
159 **sensitive to immobilized IgG/ICs.** Dose-dependent activation of FcγR-bearing reporter cells
160 by immobilized IC can be mimicked by immobilized IgG. Response curves of human FcγRIIB/C
161 and FcγRIIIA/B are similar between opsonized cells (293T cells stably expressing CD20 + Rtx),
162 immobilized IC (rec. soluble CD20 + Rtx) and immobilized IgG (Rtx). SIC formed by
163 monovalent antigen (rec. soluble CD20) do not activate human FcγRs. X-Axis shows sample
164 concentration determined by antibody molarity. Y-Axis shows FcγR activation determined by
165 reporter cell IL-2 production.
166

167 **Quantification of human FcγR responsiveness to multimeric sICs**

168 There are only few commercially available antibody-antigen pairs that meet both the above
169 mentioned high grade purity requirements while also allowing for multimeric sIC formation. We
170 focused on three pairs of multivalent antigens and their respective mAbs that were available
171 in required amounts enabling large-scale titration experiments; trimeric rhTNFα:IgG1 infliximab

172 (TNFα:Ifx), dimeric rhVEGFA: IgG1 bevacizumab (VEGFA/Bvz) and dimeric rhIL-5: IgG1
173 mepolizumab (IL-5/Mpz). As lymphocytes express TNFα-receptors I and II while not
174 expressing receptors for IL-5 or VEGFA, we tested whether our mouse lymphocyte derived
175 BW5147 thymoma reporter cell line is sensitive to high concentrations of rhTNFα. Toxicity
176 testing revealed that even high concentrations up to 76.75 nM rhTNFα did not affect viability
177 of reporter cells (Fig. S1). Next, we measured the dose-dependent activation of human FcγRs
178 comparing immobilized IgG to soluble ICs using the FcγR reporter cell panel (Fig. 3).
179 Soluble antigen or mAb alone served as negative controls showing no background activation
180 even at high concentrations. Immobilized rituximab served as a positive control for inter-
181 experimental reference. We observed that all FcγRs are strongly activated in a dose-
182 dependent manner when incubated with immobilized IgG. Incubating the FcγR reporter cells
183 with sICs at identical molarities showed FcγRIIB/C and FcγRIIIA/B to be efficiently activated
184 by sICs, while in contrast, FcγRIIA and FcγRI did not respond to sICs. We furthermore
185 observed FcγRIIIA/B to be efficiently activated by sICs with responses even surpassing those
186 achieved with immobilized IgG for TNFα/Ifx and IL-5/Mpz ICs. FcγRIIB/C showed a generally
187 weaker reactivity towards sICs compared to immobilized ICs, especially at high concentrations
188 whereas an inversion of this order was seen for TNFα/Ifx and VEGFA/Bvz ICs at lower
189 concentrations. IL-5/Mpz, FcγRIIB/C and FcγRIIIA/B showed similar responsiveness towards
190 immobilized or sICs with a generally stronger activation on immobilized ICs. These
191 experiments demonstrate that sICs of different composition vary in the resulting FcγR
192 activation pattern, most likely due to the antigens being either dimeric, trimeric or different in
193 size.

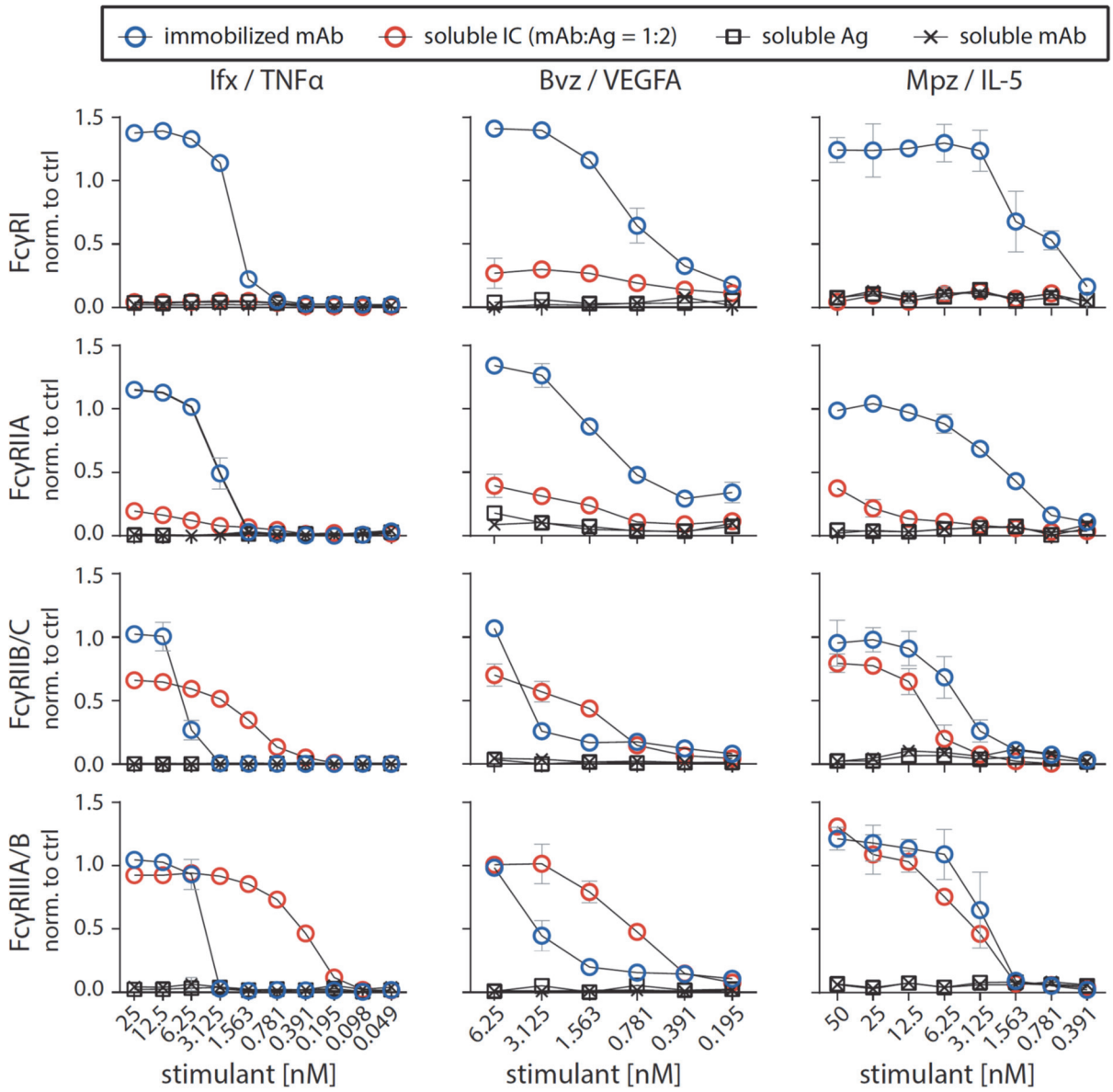

Fig. 3. FcγRIIB/C and FcγRIIIA/B are activated by sICs formed from multivalent antigens. Three different multivalent ultra-pure antigens (Ag) mixed with respective therapy-grade mAbs were used to form sICs as indicated for each set of graphs (top to bottom). IC pairs: infliximab (Ifx) and rhTNFα; mepolizumab (Mpz) and rhIL-5; bevacizumab (Bvz) and rhVEGFA. X-Axis: concentrations of stimulant expressed as molarity of either mAb or Ag monomer and IC (expressed as mAb molarity) at a mAb:Ag ratio of 1:2. Soluble antigen or soluble antibody alone served as negative controls and were not sufficient to activate human FcγRs. FcγR responses were normalized to immobilized rituximab (Rtx) at 1µg/well (set to 1) and a medium control (set to 0). All FcγRs show dose-dependent activation towards immobilized IgG. FcγRIIA shows low activation at high sIC concentrations compared to immobilized IgG activation. FcγRI shows no activation towards sICs. FcγRIIIA/B and FcγRIIB/C are dose-dependently activated by sICs with responses comparable in strength to immobilized IgG stimulant. Experiments performed in technical replicates. Error bars = SD. Error bars smaller than symbols are not shown.

210 Next, to validate the measured differences in response to sICs vs. immobilized IC for primary
211 cells, we determined FcγRIIIA activation using primary human NK cells isolated from PBMCs
212 of healthy donors. Measuring a panel of activation markers and cytokine responses by flow
213 cytometry, we observed a differential activation pattern depending on ICs being soluble or
214 immobilized at equal molarity (Fig. 4A). We chose IL-5/Mpz sICs as NK cells do not express
215 the IL-5 receptor. While MIP1-β responses were comparable between the two triggers,
216 degranulation (CD107a) and TNFα responses showed a trend towards lower activation by sICs
217 compared to immobilized IgG (Mpz). Strikingly, IFNγ responses were significantly weaker
218 when NK cells were incubated with sICs compared to immobilized IgG. In order to confirm this
219 hierarchy of responses and to enhance the overall low activation by Fcγ compared to the PMA
220 control, we changed the IC setup by generating reverse-orientation sICs consisting of human
221 FcγR-specific mAbs and goat-anti-mouse IgG $F(ab)_2$ fragments. NK cell activation by reverse
222 sICs was compared to NK cell activation by immobilized FcγR specific mAbs (Fig. 4B). Here,
223 we not only confirm our previous observations regarding MIP-1β and IFNγ, but we also confirm
224 significantly lower TNFα and CD107a responses towards soluble complexes compared to
225 immobilized mAbs. Importantly, these experiments validate that sICs readily activate primary
226 NK cells and induce immunological effector functions. As in 10% of the population NK cells
227 express FcγRIIC (Breunis et al., 2008; Metes et al., 1998), we also tested if this receptor plays
228 a role in our measurements. Using the same three donors and an FcγRII specific mAb as
229 described above, we did not observe an FcγRII-mediated response. Accordingly, we conclude
230 that FcγRIIC expression did not play a role in our experiments (Fig. 4C). Taken together, we
231 show that multivalent but not dimeric soluble immune complexes govern primary NK cell
232 response and FcγRIIIA/B activation (Fig. 2A).

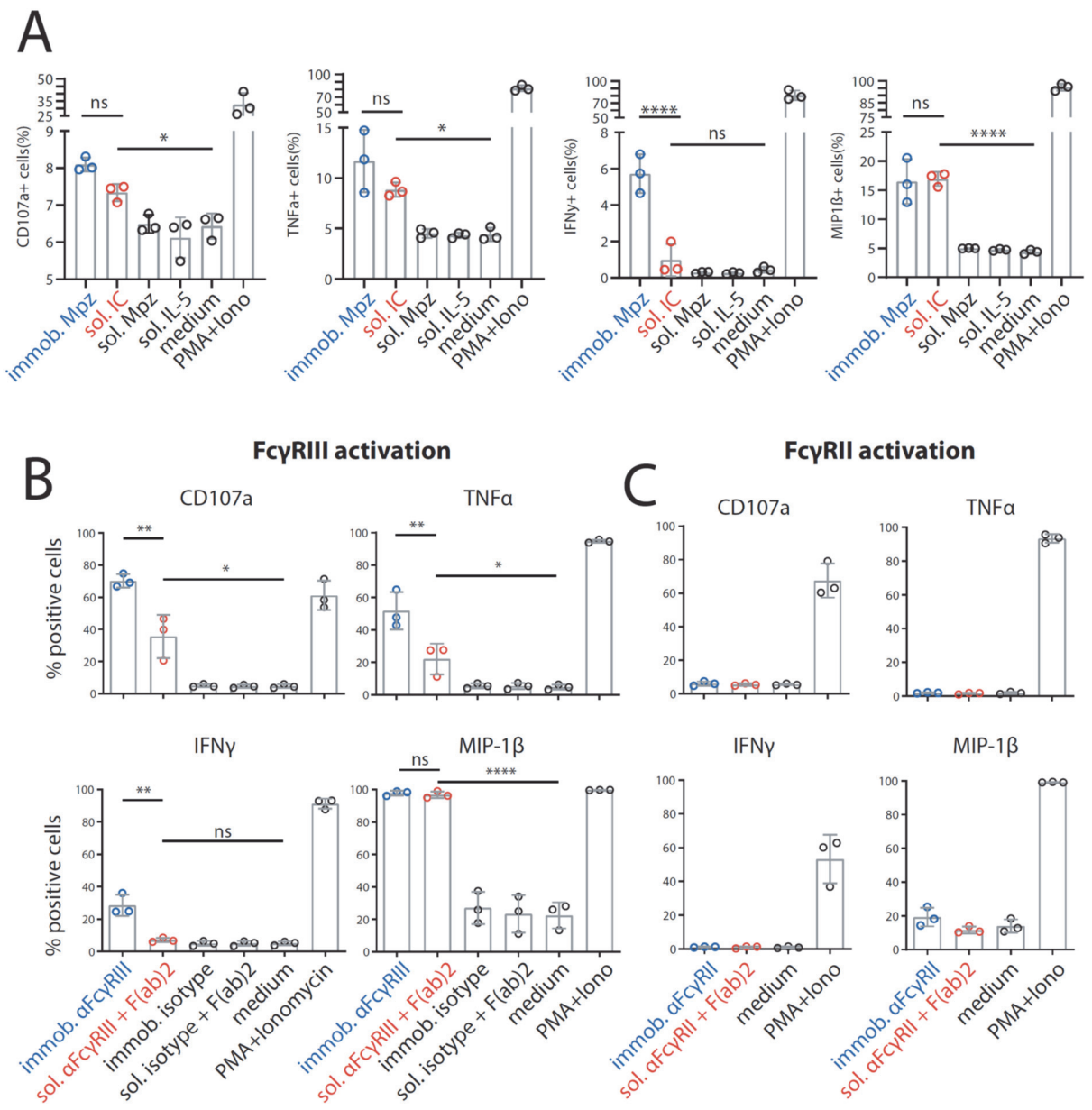

Fig. 4. The FcγRIII-dependent activation pattern of primary NK cells depends on IC solubility. Primary NK cells purified from PBMCs of three different donors were tested for NK cell activation markers. Error bars = SD. Two-way ANOVA (Turkey). A) NK cells were incubated with immobilized IgG (mepolizumab, Mpz), soluble IC (Mpz:IL-5 = 1:1), soluble Mpz or soluble IL-5 (all at 200 nM, 10^6 cells). Incubation with PMA and Ionomycin (Iono) served as a positive control. Incubation with medium alone served as a negative control. B) NK cells were incubated with immobilized FcγRIII-specific mAb, soluble mouse-anti-human IgG $F(ab)_2$ complexed FcγRIII-specific mAb (reverse sICs), immobilized IgG of non-FcγRIII-specificity (isotype control) or soluble $F(ab)_2$ complexed isotype control (all at 1µg, 10^6 cells). Incubation with PMA and Ionomycin served as a positive control. Incubation with medium alone served as a negative control. C) As in B using an FcγRII-specific mAb. NK cells from the tested donors in this study do not react to FcγRII activation.

248 **Measurement of FcγR activation in response to changing sIC size.**

249 We observed that the dimeric sIC CD20:Rtx completely failed to activate our reporter cells,
250 while potentially larger sICs based on multimeric antigens showed an efficient dose-dependent
251 FcγR activation. In order to determine whether the assay is able to respond to changes in sIC
252 size, we tested cross-titrated amounts of antibody (mAb, infliximab, Ifx) and antigen (Ag,
253 rhTNFα). To this end, the reporter cells were incubated with sIC of different mAb:Ag ratio by
254 fixing one parameter and titrating the other. According to the Heidelberger-Kendall precipitation
255 curve (Heidelberger and Kendall, 1929) describing sIC size as being dependent on the mAb:Ag
256 ratio, this should result in varying sIC sizes as an excess of either antigen or antibody results
257 in the formation of smaller complexes compared to the large molecular complexes formed at
258 around equal molarity. Changes in sIC size due to a varying mAb:Ag ratio were quantified
259 using asymmetrical flow-field flow fractionation (AF4) (Fig. 5A and Table S1). Fig. S2 shows
260 an exemplary complete run of such an analysis. AF4 analysis identifies the highest sIC mean
261 molecular being approximately 2130 kDa at a 1:3 ratio (mAb:Ag) with sICs getting smaller with
262 increasing excess of either antigen or antibody, recapitulating a Heidelberger-Kendall-like
263 curve. Incubation of the FcγR reporter cells with ICs of varying size indeed shows that the
264 assay responds to changes in sIC size (Fig. 5B). Accordingly, both FcγR types showed the
265 strongest responses at mAb:Ag ratios of approximately 1:3. We then set out to test the
266 accuracy of our reporter cell assay as a surrogate marker for primary human immune cells
267 expressing FcγRs. To this end, we isolated primary NK cells from three individual donors and
268 measured NK cell MIP1-β upregulation in response to synthetic sICs of varying size and
269 composition again using a similar assay setup optimized for NK cell activation. We chose MIP-
270 1β upregulation as a cell surface marker to measure NK cell activation as it showed the highest
271 responsiveness in previous experiments (Fig. 4). We could observe that primary immune cells
272 expressing FcγRIIIA respond to IC size, confirming our assay to be an accurate surrogate for
273 primary immune cell responses to soluble ICs (Fig. 5C). Convincingly, NK cell responses to
274 sICs generated from trimeric antigen (rhTNFα) peaked at a different mAb:Ag ratio compared
275 to NK cell responses to sICs generated from dimeric antigens (rhIL-5 and rhVEGFA). Of note,

276 TNFα and VEGFA activate resting NK cells thus leading to higher MIP1-β positivity when NK
277 cells are incubated in the presence of excess antigen. As NK cells do not express IL-5 receptor,
278 this is not observed in the presence of excess IL-5. Regarding TNFα, NK cells still show a
279 stronger activation by sICs generated under optimal mAb:Ag ratios compared to conditions
280 where excess antigen is used. This shows a clear correlation between IC size and effector
281 response. Conversely, when changing antibody concentrations using fixed amounts of antigen,
282 a consistent reduction of NK cell activation is observed in the presence of excess IgG for all
283 three mAb/Ag pairs.
284

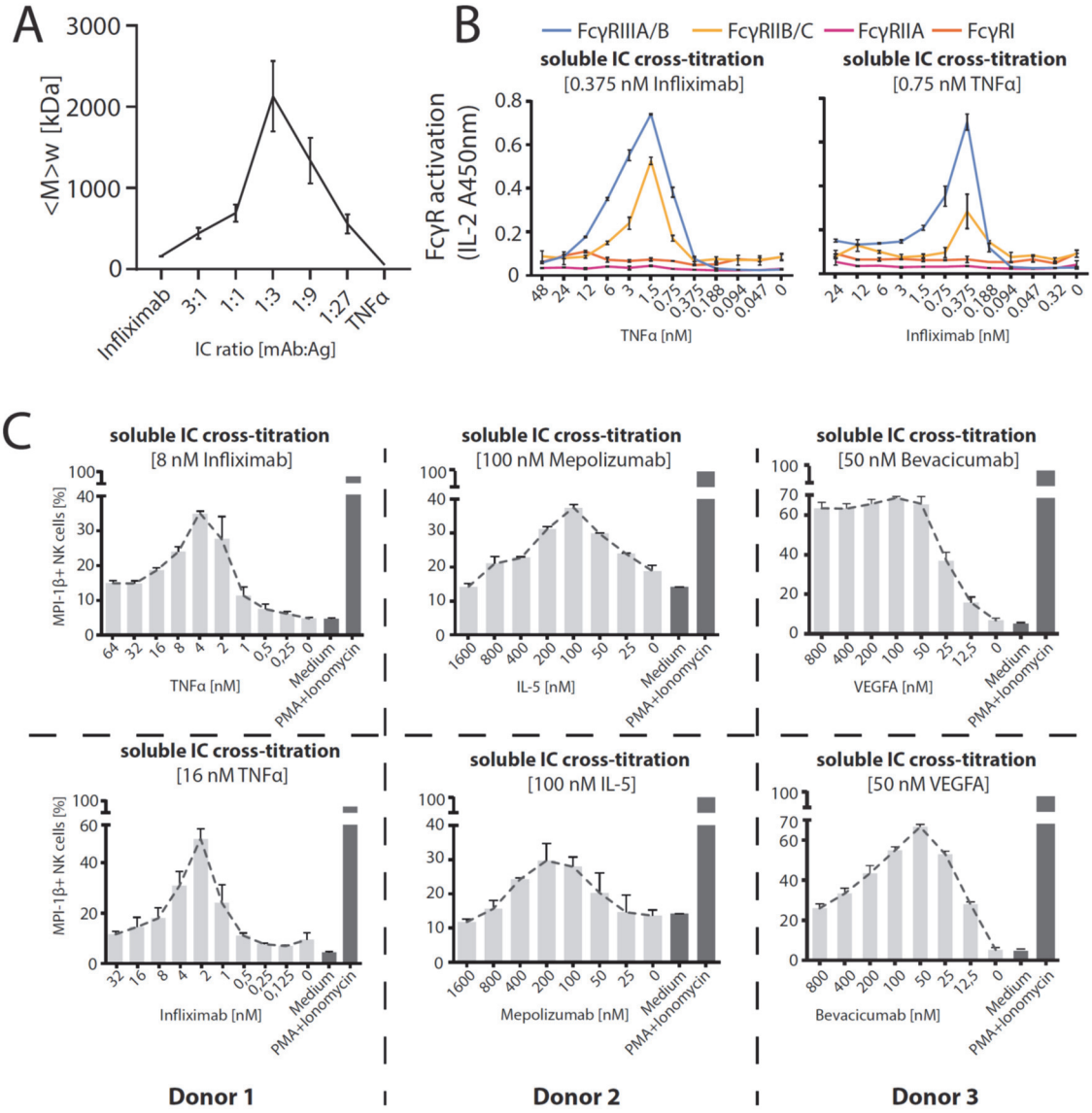

Fig. 5. The reporter assay responds to IC size reproducing a Heidelberger-Kendall like precipitation curve with a functional read-out. A) infliximab (mAb) and rhTNFα (Ag) were mixed at different ratios (17 µg total protein, calculated from monomer molarity) and analysed via AF4. sIC size is maximal at a 1:3 ratio of mAb:Ag and reduced when either mAb or Ag are given in excess. $<M>_w$ = mass-weighted mean of the molar mass distribution. Three independent experiments. Error bars = SD. Data taken from Table S1. One complete run analysis is shown in Fig. S2. B) FcγR BW5147 reporter cell activation is sensitive to sIC size. sICs of different size were generated by cross-titration according to the AF4 determination. Reporter cells were incubated with fixed amounts of either mAb (infliximab, left) or Ag (rhTNFα, right) and titrated amounts of antigen or antibody, respectively. X-Axis shows titration of either antigen or antibody, respectively (TNFα calculated as monomer). IL-2 production of reporter cells shows a peak for FcγRIIB/C and FcγRIIIA/B activation at an antibody:antigen ratio between 1:2 and 1:4. FcγRs I and IIA show no activation towards sICs in line with previous observations. Two independent experiments. Error bars = SD. C) Primary NK cells purified by negative selection magnetic bead separation from three different donors were incubated with cross-titrated sICs as in A. NK cells were measured for MIP-1β expression (% positivity). Incubation with PMA and Ionomycin served as a positive control. Incubation with medium alone served as a negative control. Measured in technical replicates. Error bars = SD.

304 **Quantification of reactive sICs in sera of SLE patients.**

305 In order to apply the assay to a clinically relevant condition we measured circulating sICs
306 present in the serum of SLE patients with variable disease activity. Sera from 4 healthy donors
307 and 25 SLE patients were investigated for FcγRIIIA/B and FcγRIIB/C activation. Reporter cells
308 produced IL-2 in response to patient sera in a dose-dependent manner (shown exemplarily for
309 one group of SLE patients in Fig. 6A), which was not the case when sera from healthy controls
310 were tested. Consistent with the observation that FcγRI and FcγRIIA do not respond to
311 synthetic sICs, reporter cells expressing these receptors did also not respond to the tested
312 serum samples. While this reaction pattern already indicated that sICs are the reactive
313 component measured in SLE patients' sera, we further demonstrate that FcγRIIIA/B and
314 FcγRIIB/C activation depends on the presence of serum ICs by analyzing patient serum before
315 and after polyethylene glycol (PEG) precipitation of sICs (Fig. 6B). Next, we calculated the
316 area under the curve (AUC) values for all 25 SLE patient titrations and normalized them to the
317 AUC values measured for healthy individuals. The resulting index values were then correlated
318 with established biomarkers of SLE disease activity, such as anti-dsDNA titers (α-dsDNA) and
319 concentrations of the complement cleavage product C3d (Fig. 6C). Both biomarkers are
320 believed to indirectly indicate the presence of sICs. We observed a significant correlation
321 between our FcγRIIIA/B activation index values and the determined disease activity markers,
322 anti-dsDNA titers and C3d ($p=0.0078$ and $p=0.0118$, respectively). FcγRIIB/C on the other
323 hand showed no significant correlation with either biomarker. We assume this may be due to
324 the influence of IgG sialyation found to be reduced in active SLE (Vuckovic et al., 2015).
325 Generally, de-sialylation of IgG leads to stronger binding by the activating receptors FcγRI,
326 FcγRIIA and FcγRIII while it reduces the binding affinity of the inhibitory FcγRIIB (Kaneko et
327 al., 2006). In sum, our assay allows the indirect quantification of clinically relevant sICs in sera
328 of SLE patients.

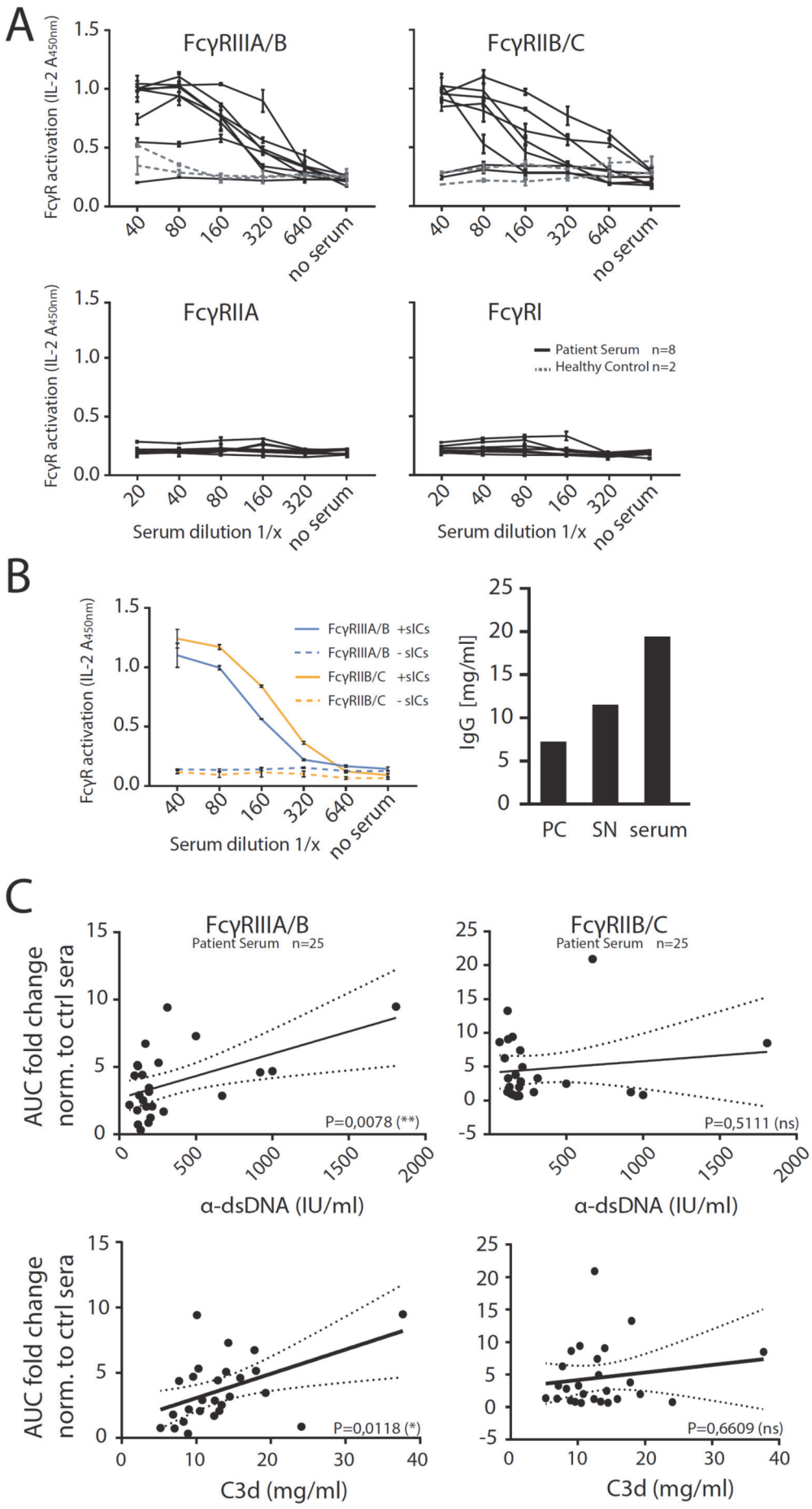
A
FcγRIIIA/B
FcγRIIB/C
FcγRIIA
FcγRI
FcγR activation (IL-2 A450nm)
Serum dilution 1/x
no serum
Patient Serum n=8
Healthy Control n=2
B
FcγRIIIA/B +sICs
FcγRIIIA/B - sICs
FcγRIIB/C +sICs
FcγRIIB/C - sICs
IgG [mg/ml]
PC
SN
serum
C
FcγRIIIA/B
Patient Serum n=25
FcγRIIB/C
Patient Serum n=25
AUC fold change norm. to ctrl sera
α-dsDNA (IU/ml)
P=0,0078 (**)
P=0,5111 (ns)
C3d (mg/ml)
P=0,0118 (*)
P=0,6609 (ns)

329

330 **Fig. 6. The reporter assay enables quantification of serum-derived sIC from SLE**
331 **patients.** Serum derived sIC from systemic lupus erythematosus (SLE) patients activate
332 human FcγR reporter cells. 25 patients and 4 healthy control individuals were separated into
333 three groups for measurement. A) Experiments shown for an exemplary group of 8 SLE
334 patients and two healthy individuals. Dose-dependent reactivity of FcγRs IIIA/B and IIB/C was
335 observed only for SLE patient sera and not for sera from healthy individuals. FcγRs I and IIA
336 show no reactivity towards clinical IC in line with previous observations. B) Activation of FcγRs
337 IIB/C and IIIA/B by patient serum is mediated by serum derived sICs. Patient serum was
338 depleted of sICs by PEG precipitation and the supernatant was compared to untreated serum
339 regarding FcγR activation (left). IgG concentration in the precipitate (SN), supernatant (SN)
340 and untreated serum is shown in the bar graph (right). IC precipitation did not remove IgG from
341 the supernatant. C) FcγRIIIA/B activation, but not FcγRIIB/C activation, significantly correlates
342 with known SLE disease markers. FcγR activation data from A was correlated to established
343 SLE disease markers (α-dsDNA levels indicated as IU/ml or C3d concentrations indicated as
344 mg/ml). FcγR activation from a dose-response curve as in A was calculated as area under
345 curve (AUC) for each SLE patient (n=25) or healthy individual (n=4) and expressed as fold
346 change compared to the healthy control mean. SLE patients with α-dsDNA levels below 50
347 IU/ml and C3d values below 9 mg/ml were excluded. Two-tailed Pearson correlation.
348

349 **Translation to clinically relevant *in vivo* lupus and arthritis mouse models.**

350 BW5147 reporter cells stably expressing chimeric mouse as well as rhesus macaque FcγRs
351 have already been generated using the here described method and were successfully used to
352 measure FcγR activation by opsonized adherent cells in previous studies (Kolb et al., 2019;
353 Van den Hoecke et al., 2017) (mFcγR reporter cells). As the human FcγR reporter cells
354 described here are sensitive to sICs, we next aimed to translate the assay to clinically relevant
355 animal models. To this end, we incubated previously described FcγR reporter cells expressing
356 chimeric mouse FcγRs (Van den Hoecke et al., 2017) with sera from lupus (NZB/WF1) or
357 arthritis (K/BxN) mice with active disease. The reporter assay was performed as described
358 above. We chose to measure the stimulation of the activating receptors, mFcγRIII and
359 mFcγRIV, that correspond to human FcγRIII and show a comparable cellular distribution and
360 immune function (Bruhns and Jonsson, 2015). Incubation with synthetic sICs generated from
361 rhTNFα and mouse-anti-hTNFα IgG1 showed both of the mFcγR reporter cells to be
362 responsive to sICs (Fig. 7A). Parental BW5147 cells expressing no FcγRs served as a negative
363 control. The sera of three mice per group were analysed and compared to sera from wildtype
364 C57BL/6 mice, which served as a negative control. We consistently detected mFcγR activation
365 by sera from K/BxN or NZB/WF1 compared to BL6 mice (Fig. 7B). While the mFcγRIII

366 responses were generally high and similar between K/BxN and NZB/WF1 mice, we found a
367 lower and more variable mFcγRIV responsiveness. We assume this might be explained by
368 differences in mFcγR affinity to mouse IgG subclasses. While mFcRIII binds IgG1, IgG2a and
369 IgG2b with comparable affinity, IgG1 is not detected by mFcRIV (Bruhns and Jonsson, 2015).
370 Further, we found that the response of mFcγRIV-expressing reporter cells shows no strict
371 dose-dependency. This effect was more pronounced for NZB/WF1 compared to K/BxN mice.
372 In addition, in this case we assume an influence of factors such as glycosylation patterns or
373 subclass composition, not further addressed here. Nevertheless, the assay enables the
374 reliable detection of sICs in sera of mice with immune-complex mediated diseases making it a
375 promising novel tool to monitor sICs as a biomarker of disease activity.

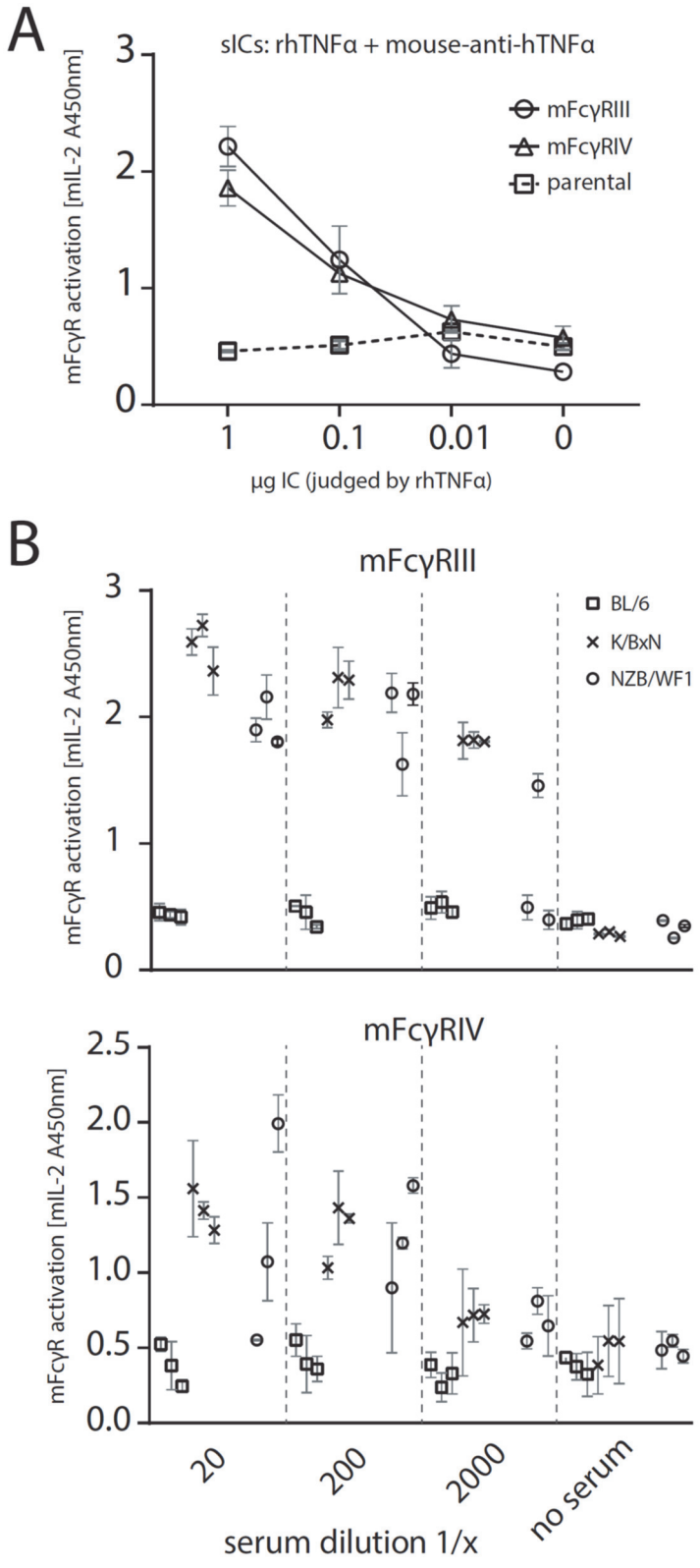

Fig. 7. The reporter assay can be translated to mouse models of autoimmune disease. A) Reporter cells expressing mFcγRIII, mFcγRIV or parental BW5147 cells were incubated with titrated amounts of synthetic sICs generated from rhTNFα and mouse-anti-hTNFα at a 1:1 ratio by mass. One experiment in technical replicates. Error bars = SD. B) Titrations of 3 mouse sera per group (BL/6, K/BxN or NZB/WF1) were incubated with mFcγR reporter cells and FcγR activation was assessed as described above. Sera from BL/6 mice served as negative control. Performed in technical replicates. Error bars = SD.

384 **Discussion**

385

386 **A novel assay for the quantification of synthetic as well as disease-associated sICs.**

387 We developed a cell-based reporter system capable of quantifying the IgG-IC mediated
388 activation of individual human and mouse FcγRs. We show that the assay is exquisitely specific
389 for immobilized ICs as well as soluble ICs. This assay presents a meaningful advancement in
390 methodology as it enables the direct detection of receptor-activating ICs. This is of great value
391 for autoimmune diseases such as systemic lupus erythematosus (SLE) and rheumatoid
392 arthritis (RA), where circulating ICs crucially contribute to disease manifestations (Koffler et al.,
393 1971; Zubler et al., 1976) and for certain infectious diseases such as COVID-19 caused by
394 SARS-CoV2 (Vuitton et al., 2020) or chronic hepatitis B virus (HBV) infection, in which
395 circulating sICs are generated (Madalinski et al., 1991; Wang and Ravetch, 2015). We
396 demonstrated that the here described assay enables quantification of serum-derived
397 circulating sICs from SLE patients with regard to FcγR reactivity. Further, the sIC-mediated
398 FcγR activation correlated with SLE disease markers. Thus, the assay may serve as promising
399 new tool to measure sIC as disease biomarker in autoimmunity or infection. We also show the
400 potential of this assay to be translated to clinically relevant animal models. As the assay also
401 enables the measurement of dose-dependent FcγR responses this allows the (semi-)
402 quantitative detection of sICs in various samples such as mAb preparations for clinical use.
403 The presence of ICs in therapeutic preparations or their formation following patient treatment
404 is unwanted due to the dangers of side effects such as lupus-like syndrome which has been
405 linked to mAb treatment in patients receiving infliximab (Wetter and Davis, 2009) or
406 bevacizumab (MacDonald et al., 2016), both mAbs used in this study. As this assay is sensitive
407 to any aggregation of IgG, it also represents a tool to control the purity and quality of mAb
408 preparations developed for therapeutic use in patients. In addition, the assessment of sIC-
409 mediated FcγR activation allows for optimization of mAb preparations targeting cytokines and
410 soluble factors, which would result in sIC formation, designed for reduced or enhanced FcγR
411 activation such as glyco-engineered mAbs or LALA-mutant mAbs (Li et al., 2017; Saunders,

412 2019). Notably, the scalability of this cell-based test system does allow for large-scale
413 screening of samples.
414
415 **FcγR activation profiles differ dependent on the solubility and size of clustered IgG.**
416 We observed a difference in the response patterns for FcγRIIIA/B and FcγRII/B/C depending
417 on the solubility of clustered IgG (immobilized versus soluble ICs) which we validated for
418 FcγRIIIA using primary human NK cells. It should be emphasized that multimeric, but not
419 dimeric sICs can trigger FcγR activation. This highlights the fundamental influence of the
420 antigen and subsequent sIC size on FcγR-dependent signal transduction. The ability of the
421 here described assay to quantify the activation of individual FcγR by sICs is not achievable
422 or directly comparable using primary cells due to non-uniform immune responses upon FcγR
423 activation and as different immune cells express FcγRs in different combinations as well as
424 variable densities. Finally, and in contrast to primary human cells, our murine reporter cells are
425 largely inert to human cytokines, which provides a key advantage to measure FcγR activation
426 selectively in response to sIC.
427 Human FcγRIIIA mediates ADCC elicited by NK cells and the induction of a pro-inflammatory
428 cytokine profile by $CD16^+$ monocytes, while FcγRIIIB is a GPI-anchored receptor on
429 neutrophils. FcγRIIB is an inhibitory receptor expressed by B cells and dendritic cells (DCs)
430 regulating B cell activation, antibody production by plasma cells and the activation state of
431 DCs, while the activating FcγRIIC is found on NK cells mediating ADCC. However, as FcγRIIC
432 is only expressed by less than 20% of the human population, its role is still poorly understood
433 (Anania et al., 2019; Lisi et al., 2011). Given the here shown difference in FcγR reactivity
434 towards multimeric sICs versus immobilized IgG it is tempting to speculate that FcγRIIIA/B-
435 and FcγRIIB/C-positive immune cells might have adapted to differentially perceive the different
436 FcγR ligands (sICs versus membrane bound insoluble ICs) and translate them into distinct
437 reaction patterns. This could be achieved by these cells via differences in receptor density,
438 signal transduction or regulation of receptor expression. Consulting the literature indeed
439 supports our hypothesis with neutrophils, B cells and NK cells being efficiently activated by

440 sICs via essentially the same receptor ectodomains (Goodier et al., 2016; Kang et al., 2016;
441 Mayadas et al., 2009; Nimmerjahn and Ravetch, 2008), while the immunological outcome of
442 their reaction very much differs.
443
444 **Revisiting the Heidelberger-Kendall curve: Dynamic sIC size measurement and**
445 **monitoring of activity in sIC-associated diseases.**
446 We provide for the first time a simultaneous functional and biophysical assessment of the
447 paradigmatic Heidelberger-Kendall precipitation curve (Heidelberger and Kendall, 1929;
448 Heidelberger and Kendall, 1935). While previous work revealed that large and small sICs show
449 differential impact on IL-6 production in PBMCs (Lux et al., 2013), the dynamics of FcγR
450 activation resulting from constant changes in sIC size have not been explored in great detail
451 yet. This was achieved in this study by directly analyzing native molecules via AF4 (Fig. 5A,
452 Fig. S2, Table S1). Our data reveal that sIC size is indeed governed by antibody:antigen ratios
453 covering a wide range of sizes up to several megadaltons. In the presence of increasing
454 amounts of antibody or antigen deviating from an optimal antibody:ratio, sIC size steadily
455 decreases. Further, by the measurement of FcγR activation we now translate sIC size directly
456 to an immunologically meaningful read-out. In doing so, we show that sIC size essentially tunes
457 FcγR activation and thereby immune cell responses. Thus, our new test system can not only
458 contribute to the functional detection and quantification of clinically relevant sICs but also
459 provides a starting point on how to avoid pathological consequences by influencing the sIC
460 size, for example by administering therapeutic antibodies or recombinant antigens in optimized
461 concentrations, thus becoming relevant in clinical pharmacokinetics.
462
463 **Limitations of the reporter system and conclusions**
464 We found that FcγRI is not activated by sICs in our assay. We assume that FcγRI activation
465 by sICs might require a native cellular environment given that a major function is the uptake of
466 ICs even in the absence of a signaling motif (Indik et al., 1994). However, we find that FcγRI
467 ectodomains alone are not responsive to sICs indicating a different cross-linking threshold for

468 FcγRI possibly linked to it being the only high-affinity FcγR with three extracellular Ig domains
469 compared to the two domains found in other FcγRs. This reflects a general consideration
470 regarding the reporter system. While providing a robust and unified read-out using a scalable
471 cell-based approach, the assay is not able to reflect native immune cell functions governed by
472 cell specific signalling cascades. The major advancements of this reporter system include i) a
473 higher accuracy regarding FcγR activation compared to strict affinity measurement, ii) an sIC
474 size dependent quantification of FcγR responsiveness and iii) the identification of FcγR
475 activating sICs in autoimmunity but also infection. Finally, this scalable, sensitive and robust
476 system to detect FcγR activating sICs in clinical samples might enable their identification
477 diseases that have not been linked to sIC-mediated pathology, yet.
478

479 **Materials and Methods**

480

481 **Cell culture**

482 All cells were cultured in a 5% CO_2 atmosphere at 37°C. BW5147 mouse thymoma cells (BW,
483 obtained from ATCC: TIB-47) were maintained at $3x10^5$ to $9x10^5$ cells/ml in Roswell Park
484 Memorial Institute medium (RPMI GlutaMAX, Gibco) supplemented with 10% (vol/vol) fetal calf
485 serum (FCS, Biochrom), sodium pyruvate (1x, Gibco) and β-mercaptoethanol (0.1 mM, Gibco).
486 293T-CD20 (kindly provided by Irvin Chen, UCLA (Morizono et al., 2010)) were maintained in
487 Dulbecco's modified Eagle's medium (DMEM, Gibco) supplemented with 10% (vol/vol) FCS.
488

489 **FcγR receptor activation assay**

490 FcγR activation was measured adapting a previously described cell-based assay (Corrales-
491 Aguilar et al., 2014; Corrales-Aguilar et al., 2013). The assay was modified to measure FcγR
492 activation in solution. Briefly, $2x10^5$ BW-FcγR (BW5147) reporter cells were incubated with
493 synthetic sIC in a total volume of 100 µl for 16 h at 37°C and 5% CO_2. Incubation was performed
494 in a 96-well ELISA plate (Nunc maxisorp) pre-treated with PBS/10% FCS (v/v) for 1 h at 4°C.
495 Immobilized IgG was incubated in PBS on the plates prior to PBS/10% FCS treatment.

496 Reporter cell mIL-2 secretion was quantified via ELISA as described previously (Corrales-
497 Aguilar et al., 2013).
498
499 **Recombinant antigens and monoclonal antibodies to form sICs**
500 Recombinant human (rh) cytokines TNF, IL-5, and VEGFA were obtained from Stem Cell
501 technologies. Recombinant CD20 was obtained as a peptide (aa141-188) containing the
502 binding region of rituximab (Creative Biolabs). FcγR-specific mAbs were obtained from Stem
503 Cell technologies (CD16: clone 3G8; CD32: IV.3). Reverse sICs were generated from these
504 receptor-specific antibodies using goat-anti-mouse IgG $F(ab)_2$ fragments (Invitrogen) in a 1:1
505 ratio. Pharmaceutically produced humanized monoclonal IgG1 antibodies infliximab (Ifx),
506 bevacizumab (Bvz), mepolizumab (Mpz) and rituximab (Rtx) were obtained from the University
507 Hospital Pharmacy Freiburg. Mouse anti-hTNFα (IgG2b, R&D Systems, 983003) was used to
508 generate sICs reactive with mouse FcγRs. sICs were generated by incubation of antigens and
509 antibodies in reporter cell medium or PBS for 2 h at 37°C.
510
511 **Lentiviral transduction**
512 Lentiviral transduction was performed as described previously (Kolb et al., 2019; Van den
513 Hoecke et al., 2017). In brief, chimeric FcγR-CD3ζ constructs (Corrales-Aguilar et al., 2013)
514 were cloned into a pUC2CL6IPwo plasmid backbone. For every construct, one 10-cm dish of
515 packaging cell line at roughly 70% density was transfected with the target construct and two
516 supplementing vectors providing the VSV gag/pol and VSV-G-env proteins (6 µg of DNA each)
517 using polyethylenimine (22.5 µg/ml, Sigma) and Polybrene (4 µg/ml; Merck Millipore) in a total
518 volume of 7 ml (2 ml of a 15-min-preincubated transfection mix in serum-free DMEM added to
519 5 ml of fresh full DMEM). After a medium change, virus supernatant harvested from the
520 packaging cell line 2 days after transfection was then incubated with target BW cells overnight
521 (3.5 ml of supernatant on 10^6 target cells), followed by expansion and pool selection using
522 complete medium supplemented with 2 µg/ml of puromycin (Sigma) over a one week culture
523 period.

524

525 **BW5147 toxicity test**

526 Cell counting was performed using a Countess II (Life Technologies) according to supplier
527 instructions. Cell toxicity was measured as a ratio between live and dead cells judged by trypan
528 blue staining over a 16 h time frame in a 96well format (100 µl volume per well). BW5147 cells
529 were mixed 1:1 with Trypan blue (Invitrogen) and analysed using a Countess II. rhTNFα was
530 diluted in complete medium.

531

532 **human IgG suspension ELISA**

533 1 µg of IgG1 (rituximab in PBS, 50 µl/well) per well was incubated on a 96well microtiter plate
534 (NUNC Maxisorp) pre-treated (2h at RT) with PBS supplemented with varying percentages
535 (v/v) of FCS (PAN Biotech). IgG1 bound to the plates was detected using an HRP-conjugated
536 mouse-anti-human IgG mAb (Jackson ImmunoResearch).

537

538 **BW5147 cell flow cytometry**

539 BW5147 cells were harvested by centrifugation at 900 g and RT from the suspension culture.
540 $1x10^6$ cells were stained with PE- or FITC-conjugated anti-human FcγR mAbs (BD) or a PE-
541 TexasRed-conjugated human IgG-Fc fragment (Rockland) for 1h at 4°C in PBS/3%FCS. After
542 3 washing steps in PBS/3%FCS, the cells were transferred to Flow cytometry tubes (BD) and
543 analysed using BD LSR Fortessa and FlowJo (V10) software.

544

545 **NK cell activation flow cytometry**

546 PBMC were purified from donor blood using Lymphocyte separation Media (Anprotec). Primary
547 NK cells were separated from donor PBMCs via magnetic bead negative selection (Stem Cell
548 technologies). 96well ELISA plates (Nunc Maxisorp) were pre-treated with PBS/10% FCS (v/v)
549 for 1 h at 4°C. NK cells were stimulated in pre-treated plates and incubated at 37°C and 5%
550 CO_2 for 4 h. Golgi Plug and Golgi Stop solutions (BD) were added as suggested by supplier.
551 CD107a (APC, BD, H4A3) specific conjugated mAb was added at the beginning of the

552 incubation period. Following the stimulation period, MIP-1β (PE, BD Pharmigen), IFNγ (BV-
553 510, Biolegends, 4SB3) and TNFα (PE/Cy7, Biolegends, MAB11) production was measured
554 via intracellular staining Cytokines (BD, CytoFix/CytoPerm, Kit as suggested by the supplier).
555 50 ng/ml PMA (InvivoGen) + 0.5 µM Ionomycin (InvivoGen) were used as a positive stimulation
556 control for NK cell activation. After 3 washing steps in PBS/3%FCS, the cells were transferred
557 to Flow cytometry tubes (BD) and analysed using a BD FACS Fortessa and FlowJo (V10)
558 software. FcγRII or FcγRIII block was performed by addition of receptor specific mAbs (Stem
559 cell technologies, IV.3 and 3G8) at a 1:100 dilution at the beginning of the incubation period.
560 Cells were transferred to Flow cytometry tubes (BD) and analyzed using BD LSR Fortessa and
561 FlowJo (V10) software.
562
563 **Asymmetric flow field flow fractionation (AF4)**
564 The AF4 system consisted of a flow controller (Eclipse AF4, Wyatt), a MALS detector (DAWN
565 Heleos II, Wyatt), a UV detector (1260 Infinity G1314F, Agilent) and the separation channel
566 (SC channel, PES membrane, cut-off 10 kDa, 490 µm spacer, wide type, Wyatt). Elution buffer:
567 1.15 g/L Na_2HPO_4 (Merck), 0.20 g/L NaH_2PO_4 x H_2O (Merck), 8.00 g/L NaCl (Sigma) and 0,20
568 g/L NaN_3 (Sigma), adjusted to pH 7.4, filtered through 0.1 µm. AF4 sequence (Vx = cross flow
569 in mL/min): (a) elution (2 min, Vx: 1.0); (b) focus (1 min, Vx: 1.0), focus + inject (1 min, Vx: 1.0,
570 inject flow: 0.2 mL/min), repeated three times; (c) elution (30 min, linear Vx gradient: 1.0 to
571 0.0); (d) elution (15 min, Vx: 0.0); (e) elution + inject (5 min, Vx: 0.0). A total protein mass of
572 17±0.3 µg (Ifx, rhTNFα or ICs, respectively) was injected. The eluted sample concentration
573 was calculated from the UV signal at 280 nm using extinction coefficients of 1.240 mL/(mg cm)
574 or 1.450 mL/(mg cm) in the case of TNFα or Ifx, respectively. For the ICs, extinction coefficients
575 were not available and difficult to calculate as the exact stoichiometry is not known. An
576 extinction coefficient of 1.450 mL/(mg cm) was used for calculating the molar masses of all
577 ICs. Especially in the case of ICs rich in TNFα, the true coefficients should be lower, and the
578 molar masses of these complexes are overestimated by not more than 14 %. The determined
579 molar masses for TNFα-rich complexes are therefore biased but the observed variations in

580 molar mass for the different ICs remain valid. The mass-weighted mean of the distribution of
581 molar masses for each sample was calculated using the ASTRA 7 software package (Wyatt).
582
583 **SLE patient cohort**
584 Sera from patients with SLE were provided by the ImmRheum biobank of the Department of
585 Rheumatology and Clinical Immunology. Biobanking and the project were approved by the
586 local ethical committee of the University of Freiburg (votes 507/16 and 624/14). All patients
587 who provided blood to the biobank had provided written informed consent. Ethical Statement:
588 The study was designed in accordance with the guidelines of the Declaration of Helsinki
589 (revised 2013). Patients with SLE (*n* = 25) and healthy controls (*n* = 4) were examined. All
590 patients met the revised ACR classification criteria for SLE. Disease activity was assessed
591 using the SLEDAI-2K score. Serum concentrations of anti–double-stranded DNA (α-dsDNA)
592 and the complement cleavage product Cd3 were monitored and indicated as IU/ml and mg/ml,
593 respectively. Anti-dsDNA concentrations in units and C3d concentrations provide sensitive
594 markers for disease activity in SLE.
595
596 **Patient serum IC precipitation**
597 For polyethylene glycol (PEG) precipitation human sera were mixed with PEG 6000 (Sigma-
598 Aldrich) in PBS at a final concentration of 10% PEG 6000. After overnight incubation at 4°C,
599 ICs were precipitated by centrifugation at 2000 x g for 30 min at 4 °C, pellets were washed
600 once with PEG 6000 and then centrifugated at 2000 x g for 20 min at 4 °C. Supernatants were
601 harvested and precipitates re-suspended in pre-warmed PBS for 1 h at 37 °C. IgG
602 concentrations of serum, precipitates and supernatants obtained after precipitation were
603 quantified by Nanodrop (Thermo Scientific™) measurement.
604
605 **Mice and Models**
606 Animal experiments were approved by the local governmental commission for animal
607 protection of Freiburg (Regierungspräsidium Freiburg, approval no. G16/59 and G19/21).

608 Lupus-prone (NZBxNZW)F1 mice (NZB/WF1) were generated by crossing NZB/BINJ mice with
609 NZW/LacJ mice, purchased from The Jackson Laboratory. KRNtg mice were obtained from F.
610 Nimmerjahn (Universität Erlangen-Nürnberg) with the permission of D. Mathis and C. Benoist
611 (Harvard Medical School, Boston, MA), C57BL/6 mice (BL/6) and NOD/ShiLtJArc (NOD/Lt)
612 mice were obtained from the Charles River Laboratories. K/BxN (KRNtgxNOD)F1 mice
613 (K/BxN) were obtained by crossing KRNtg mice and NOD/Lt mice. All mice were housed in a
614 12-h light/dark cycle, with food and water ad libitum. Mice were euthanized and blood collected
615 for serum preparation from 16 weeks old BL/6 animals, from 16 weeks old arthritic K/BxN
616 animals and from 26 – 38 weeks old NZB/WF1 mice with established glomerulonephritis.
617

618 **Statistical analyses**

619 Statistical analyses were performed using Graphpad Prism software (v6) and appropriate
620 tests.
621

622 **Funding**

623 This work was supported by an intramural junior investigator fund of the Faculty of Medicine
624 to PK (EQUIP - Funding for Medical Scientists, Faculty of Medicine, University of Freiburg), by
625 the German Research foundation (DFG) (FOR2830 HE 2526/9-1) to HH, by the DFG research
626 grant TRR130 to REV and the Ministry of Science, Research, and Arts Baden-Württemberg
627 (Margarete von Wrangell Programm) to NC.
628

629 **Acknowledgement**

630 We thank T. Schleyer (ImmRheum Biobank) for providing patient samples.
631

632 **Competing interests**

633 We declare no financial and non-financial competing interests.
634
635
636

637 **References**

638 Anania, J.C., A.M. Chenoweth, B.D. Wines, and P.M. Hogarth. 2019. The Human FcgammaRII
639 (CD32) Family of Leukocyte FcR in Health and Disease. *Front Immunol* 10:464.
640 Antes, U., H.P. Heinz, D. Schultz, D. Brackertz, and M. Loos. 1991. C1q-bearing immune
641 complexes detected by a monoclonal antibody to human C1q in rheumatoid arthritis
642 sera and synovial fluids. *Rheumatol Int* 10:245-250.
643 Bano, A., A. Pera, A. Almoukayed, T.H.S. Clarke, S. Kirmani, K.A. Davies, and F. Kern. 2019.
644 CD28 (null) CD4 T-cell expansions in autoimmune disease suggest a link with
645 cytomegalovirus infection. *F1000Res* 8:
646 Berger, S., H. Ballo, and H.J. Stutte. 1996. Immune complex-induced interleukin-6, interleukin-
647 10 and prostaglandin secretion by human monocytes: A network of pro- and anti-
648 inflammatory cytokines dependent on the antigen:antibody ratio. *Eur J Immunol*
649 26:1297-1301.
650 Bohm, S., D. Kao, and F. Nimmerjahn. 2014. Sweet and sour: the role of glycosylation for the
651 anti-inflammatory activity of immunoglobulin G. *Current topics in microbiology and*
652 *immunology* 382:393-417.
653 Bournazos, S., T.T. Wang, R. Dahan, J. Maamary, and J.V. Ravetch. 2017. Signaling by
654 Antibodies: Recent Progress. *Annu Rev Immunol* 35:285-311.
655 Breunis, W.B., E. van Mirre, M. Bruin, J. Geissler, M. de Boer, M. Peters, D. Roos, M. de Haas,
656 H.R. Koene, and T.W. Kuijpers. 2008. Copy number variation of the activating FCGR2C
657 gene predisposes to idiopathic thrombocytopenic purpura. *Blood* 111:1029-1038.
658 Bruhns, P. 2012. Properties of mouse and human IgG receptors and their contribution to
659 disease models. *Blood* 119:5640-5649.
660 Bruhns, P., B. Iannascoli, P. England, D.A. Mancardi, N. Fernandez, S. Jorieux, and M.
661 Daeron. 2009a. Specificity and affinity of human Fc gamma receptors and their
662 polymorphic variants for human IgG subclasses. *Blood* 113:3716-3725.
663 Bruhns, P., B. Iannascoli, P. England, D.A. Mancardi, N. Fernandez, S. Jorieux, and M.
664 Daeron. 2009b. Specificity and affinity of human Fcgamma receptors and their
665 polymorphic variants for human IgG subclasses. *Blood* 113:3716-3725.
666 Bruhns, P., and F. Jonsson. 2015. Mouse and human FcR effector functions. *Immunol Rev*
667 268:25-51.
668 Corrales-Aguilar, E., M. Trilling, K. Hunold, M. Fiedler, V.T. Le, H. Reinhard, K. Ehrhardt, E.
669 Merce-Maldonado, E. Aliyev, A. Zimmermann, D.C. Johnson, and H. Hengel. 2014.
670 Human cytomegalovirus Fcgamma binding proteins gp34 and gp68 antagonize
671 Fcgamma receptors I, II and III. *PLoS pathogens* 10:e1004131.
672 Corrales-Aguilar, E., M. Trilling, H. Reinhard, E. Merce-Maldonado, M. Widera, H. Schaal, A.
673 Zimmermann, O. Mandelboim, and H. Hengel. 2013. A novel assay for detecting virus-
674 specific antibodies triggering activation of Fcgamma receptors. *Journal of*
675 *immunological methods* 387:21-35.
676 Duchemin, A.M., L.K. Ernst, and C.L. Anderson. 1994. Clustering of the High-Affinity Fc
677 Receptor for Immunoglobulin-G (Fc-Gamma-Ri) Results in Phosphorylation of Its
678 Associated Gamma-Chain. *J Biol Chem* 269:12111-12117.
679 Fossati, G., R.C. Bucknall, and S.W. Edwards. 2002a. Insoluble and soluble immune
680 complexes activate neutrophils by distinct activation mechanisms: changes in
681 functional responses induced by priming with cytokines. *Ann Rheum Dis* 61:13-19.
682 Fossati, G., R.C. Bucknall, and S.W. Edwards. 2002b. Insoluble and soluble immune
683 complexes activate neutrophils by distinct activation mechanisms: changes in
684 functional responses induced by priming with cytokines. *Ann Rheum Dis* 61:13-19.
685 Getahun, A., and J.C. Cambier. 2015. Of ITIMs, ITAMs, and ITAMis: revisiting immunoglobulin
686 Fc receptor signaling. *Immunol Rev* 268:66-73.
687 Goodier, M.R., C. Lusa, S. Sherratt, A. Rodriguez-Galan, R. Behrens, and E.M. Riley. 2016.
688 Sustained Immune Complex-Mediated Reduction in CD16 Expression after
689 Vaccination Regulates NK Cell Function. *Front Immunol* 7:384.

690 Granger, V., M. Peyneau, S. Chollet-Martin, and L. de Chaisemartin. 2019. Neutrophil
691 Extracellular Traps in Autoimmunity and Allergy: Immune Complexes at Work. *Front*
692 *Immunol* 10:2824.
693 Greenberg, S., P. Chang, and S.C. Silverstein. 1994. Tyrosine phosphorylation of the gamma
694 subunit of Fc gamma receptors, p72syk, and paxillin during Fc receptor-mediated
695 phagocytosis in macrophages. *J Biol Chem* 269:3897-3902.
696 Guilliams, M., P. Bruhns, Y. Saeys, H. Hammad, and B.N. Lambrecht. 2014. The function of
697 Fcgamma receptors in dendritic cells and macrophages. *Nat Rev Immunol* 14:94-108.
698 Heidelberger, M., and F.E. Kendall. 1929. A Quantitative Study of the Precipitin Reaction
699 between Type Iii Pneumococcus Polysaccharide and Purified Homologous Antibody. *J*
700 *Exp Med* 50:809-823.
701 Heidelberger, M., and F.E. Kendall. 1935. The Precipitin Reaction between Type Iii
702 Pneumococcus Polysaccharide and Homologous Antibody : Iii. A Quantitative Study
703 and a Theory of the Reaction Mechanism. *J Exp Med* 61:563-591.
704 Hubbard, J.J., M. Pyzik, T. Rath, L.K. Kozicky, K.M.K. Sand, A.K. Gandhi, A. Grevys, S. Foss,
705 S.C. Menzies, J.N. Glickman, E. Fiebiger, D.C. Roopenian, I. Sandlie, J.T. Andersen,
706 L.M. Sly, K. Baker, and R.S. Blumberg. 2020. FcRn is a CD32a coreceptor that
707 determines susceptibility to IgG immune complex-driven autoimmunity. *J Exp Med* 217:
708 Indik, Z.K., S. Hunter, M.M. Huang, X.Q. Pan, P. Chien, C. Kelly, A.I. Levinson, R.P. Kimberly,
709 and A.D. Schreiber. 1994. The high affinity Fc gamma receptor (CD64) induces
710 phagocytosis in the absence of its cytoplasmic domain: the gamma subunit of Fc
711 gamma RIIIA imparts phagocytic function to Fc gamma RI. *Exp Hematol* 22:599-606.
712 Kaneko, Y., F. Nimmerjahn, and J.V. Ravetch. 2006. Anti-inflammatory activity of
713 immunoglobulin G resulting from Fc sialylation. *Science* 313:670-673.
714 Kang, S., A.B. Keener, S.Z. Jones, R.J. Benschop, A. Caro-Maldonado, J.C. Rathmell, S.H.
715 Clarke, G.K. Matsushima, J.K. Whitmire, and B.J. Vilen. 2016. IgG-Immune Complexes
716 Promote B Cell Memory by Inducing BAFF. *J Immunol* 196:196-206.
717 Kiefer, F., J. Brumell, N. Al-Alawi, S. Latour, A. Cheng, A. Veillette, S. Grinstein, and T.
718 Pawson. 1998. The Syk protein tyrosine kinase is essential for Fc gamma receptor
719 signaling in macrophages and neutrophils. *Mol Cell Biol* 18:4209-4220.
720 Koenderman, L. 2019. Inside-Out Control of Fc-Receptors. *Front Immunol* 10:544.
721 Koffler, D., V. Agnello, R. Thoburn, and H.G. Kunkel. 1971. Systemic lupus erythematosus:
722 prototype of immune complex nephritis in man. *J Exp Med* 134:169-179.
723 Kolb, P., S. Sijmons, M.R. McArdle, H. Taher, J. Womack, C. Hughes, A. Ventura, M.A. Jarvis,
724 C. Stahl-Hennig, S. Hansen, L.J. Picker, D. Malouli, H. Hengel, and K. Fruh. 2019.
725 Identification and Functional Characterization of a Novel Fc Gamma-Binding
726 Glycoprotein in Rhesus Cytomegalovirus. *J Virol* 93:
727 Laborde, E.A., S. Vanzulli, M. Beigier-Bompadre, M.A. Isturiz, R.A. Ruggiero, M.G. Fourcade,
728 A.C. Catalan Pellet, S. Sozzani, and M. Vulcano. 2007. Immune complexes inhibit
729 differentiation, maturation, and function of human monocyte-derived dendritic cells. *J*
730 *Immunol* 179:673-681.
731 Lagasse, H.A.D., H. Hengel, B. Golding, and Z.E. Sauna. 2019. Fc-Fusion Drugs Have
732 FcgammaR/C1q Binding and Signaling Properties That May Affect Their
733 Immunogenicity. *AAPS J* 21:62.
734 Li, T., D.J. DiLillo, S. Bournazos, J.P. Giddens, J.V. Ravetch, and L.X. Wang. 2017. Modulating
735 IgG effector function by Fc glycan engineering. *Proceedings of the National Academy*
736 *of Sciences of the United States of America* 114:3485-3490.
737 Lisi, S., M. Sisto, D.D. Lofrumento, S. D'Amore, and M. D'Amore. 2011. Advances in the
738 understanding of the Fc gamma receptors-mediated autoantibodies uptake. *Clin Exp*
739 *Med* 11:1-10.
740 Lu, L.L., T.J. Suscovich, S.M. Fortune, and G. Alter. 2018. Beyond binding: antibody effector
741 functions in infectious diseases. *Nat Rev Immunol* 18:46-61.
742 Luo, Y., J.W. Pollard, and A. Casadevall. 2010. Fcgamma receptor cross-linking stimulates
743 cell proliferation of macrophages via the ERK pathway. *J Biol Chem* 285:4232-4242.
744 Lux, A., X. Yu, C.N. Scanlan, and F. Nimmerjahn. 2013. Impact of immune complex size and
745 glycosylation on IgG binding to human FcgammaRs. *J Immunol* 190:4315-4323.

746 MacDonald, D.A., J. Martin, K.K. Muthusamy, J.K. Luo, E. Pyles, A. Rafique, T. Huang, T.
747 Potocky, Y. Liu, J. Cao, F. Bono, N. Delesque, P. Savi, J. Francis, A. Amirkhosravi, T.
748 Meyer, C. Romano, M. Glinka, G.D. Yancopoulos, N. Stahl, S.J. Wiegand, and N.
749 Papadopoulos. 2016. Aflibercept exhibits VEGF binding stoichiometry distinct from
750 bevacizumab and does not support formation of immune-like complexes. *Angiogenesis*
751 19:389-406.
752 Madalinski, K., B. Burczynska, K.H. Heermann, A. Uy, and W.H. Gerlich. 1991. Analysis of
753 viral proteins in circulating immune complexes from chronic carriers of hepatitis B virus.
754 *Clin Exp Immunol* 84:493-500.
755 Mathsson, L., E. Ahlin, C. Sjowall, T. Skogh, and J. Ronnelid. 2007. Cytokine induction by
756 circulating immune complexes and signs of in-vivo complement activation in systemic
757 lupus erythematosus are associated with the occurrence of anti-Sjogren's syndrome A
758 antibodies. *Clin Exp Immunol* 147:513-520.
759 Mayadas, T.N., G.C. Tsokos, and N. Tsuboi. 2009. Mechanisms of immune complex-mediated
760 neutrophil recruitment and tissue injury. *Circulation* 120:2012-2024.
761 Metes, D., L.K. Ernst, W.H. Chambers, A. Sulica, R.B. Herberman, and P.A. Morel. 1998.
762 Expression of functional CD32 molecules on human NK cells is determined by an allelic
763 polymorphism of the FcgammaRIIC gene. *Blood* 91:2369-2380.
764 Morizono, K., A. Ku, Y. Xie, A. Harui, S.K. Kung, M.D. Roth, B. Lee, and I.S. Chen. 2010.
765 Redirecting lentiviral vectors pseudotyped with Sindbis virus-derived envelope proteins
766 to DC-SIGN by modification of N-linked glycans of envelope proteins. *J Virol* 84:6923-
767 6934.
768 Nimmerjahn, F., and J.V. Ravetch. 2006. Fcgamma receptors: old friends and new family
769 members. *Immunity* 24:19-28.
770 Nimmerjahn, F., and J.V. Ravetch. 2008. Fcgamma receptors as regulators of immune
771 responses. *Nat Rev Immunol* 8:34-47.
772 Nimmerjahn, F., and J.V. Ravetch. 2010. Antibody-mediated modulation of immune
773 responses. *Immunol Rev* 236:265-275.
774 Patel, K.R., J.T. Roberts, and A.W. Barb. 2019. Multiple Variables at the Leukocyte Cell
775 Surface Impact Fc gamma Receptor-Dependent Mechanisms. *Front Immunol* 10:223.
776 Pierson, T.C., Q. Xu, S. Nelson, T. Oliphant, G.E. Nybakken, D.H. Fremont, and M.S.
777 Diamond. 2007. The stoichiometry of antibody-mediated neutralization and
778 enhancement of West Nile virus infection. *Cell Host Microbe* 1:135-145.
779 Pincetic, A., S. Bournazos, D.J. DiLillo, J. Maamary, T.T. Wang, R. Dahan, B.M. Fiebiger, and
780 J.V. Ravetch. 2014. Type I and type II Fc receptors regulate innate and adaptive
781 immunity. *Nat Immunol* 15:707-716.
782 Plomp, R., L.R. Ruhaak, H.W. Uh, K.R. Reiding, M. Selman, J.J. Houwing-Duistermaat, P.E.
783 Slagboom, M. Beekman, and M. Wuhrer. 2017. Subclass-specific IgG glycosylation is
784 associated with markers of inflammation and metabolic health. *Sci Rep* 7:12325.
785 Ravetch, J.V., and S. Bolland. 2001. IgG Fc receptors. *Annu Rev Immunol* 19:275-290.
786 Saunders, K.O. 2019. Conceptual Approaches to Modulating Antibody Effector Functions and
787 Circulation Half-Life. *Front Immunol* 10:1296.
788 Tahir, S., Y. Fukushima, K. Sakamoto, K. Sato, H. Fujita, J. Inoue, T. Uede, Y. Hamazaki, M.
789 Hattori, and N. Minato. 2015. A CD153+CD4+ T follicular cell population with cell-
790 senescence features plays a crucial role in lupus pathogenesis via osteopontin
791 production. *J Immunol* 194:5725-5735.
792 Tanaka, M., S.R. Krutzik, P.A. Sieling, D.J. Lee, T.H. Rea, and R.L. Modlin. 2009. Activation
793 of Fc gamma RI on monocytes triggers differentiation into immature dendritic cells that
794 induce autoreactive T cell responses. *J Immunol* 183:2349-2355.
795 Tay, M.Z., K. Wiehe, and J. Pollara. 2019. Antibody-Dependent Cellular Phagocytosis in
796 Antiviral Immune Responses. *Front Immunol* 10:332.
797 Urlaub, D., S. Zhao, N. Blank, R. Bergner, M. Claus, T. Tretter, H.M. Lorenz, C. Watzl, and W.
798 Merkt. 2019. Activation of natural killer cells by rituximab in granulomatosis with
799 polyangiitis. *Arthritis Res Ther* 21:277.
800 Van den Hoecke, S., K. Ehrhardt, A. Kolpe, K. El Bakkouri, L. Deng, H. Grootaert, S.
801 Schoonooghe, A. Smet, M. Bentahir, K. Roose, M. Schotsaert, B. Schepens, N.

802 Callewaert, F. Nimmerjahn, P. Staeheli, H. Hengel, and X. Saelens. 2017. Hierarchical
803 and Redundant Roles of Activating FcgammaRs in Protection against Influenza
804 Disease by M2e-Specific IgG1 and IgG2a Antibodies. *J Virol* 91:
805 van der Poel, C.E., R.M. Spaapen, J.G. van de Winkel, and J.H. Leusen. 2011. Functional
806 characteristics of the high affinity IgG receptor, FcgammaRI. *J Immunol* 186:2699-
807 2704.
808 Vidarsson, G., G. Dekkers, and T. Rispens. 2014. IgG subclasses and allotypes: from structure
809 to effector functions. *Front Immunol* 5:520.
810 Vogelpoel, L.T., D.L. Baeten, E.C. de Jong, and J. den Dunnen. 2015. Control of cytokine
811 production by human fc gamma receptors: implications for pathogen defense and
812 autoimmunity. *Front Immunol* 6:79.
813 Vuckovic, F., J. Kristic, I. Gudelj, M. Teruel, T. Keser, M. Pezer, M. Pucic-Bakovic, J. Stambuk,
814 I. Trbojevic-Akmacic, C. Barrios, T. Pavic, C. Menni, Y. Wang, Y. Zhou, L. Cui, H. Song,
815 Q. Zeng, X. Guo, B.A. Pons-Estel, P. McKeigue, A. Leslie Patrick, O. Gornik, T.D.
816 Spector, M. Harjacek, M. Alarcon-Riquelme, M. Molokhia, W. Wang, and G. Lauc.
817 2015. Association of systemic lupus erythematosus with decreased
818 immunosuppressive potential of the IgG glycome. *Arthritis Rheumatol* 67:2978-2989.
819 Vuitton, D.A., L. Vuitton, E. Seilles, and P. Galanaud. 2020. A plea for the pathogenic role of
820 immune complexes in severe Covid-19. *Clin Immunol* 217:108493.
821 Wang, T.T., and J.V. Ravetch. 2015. Immune complexes: not just an innocent bystander in
822 chronic viral infection. *Immunity* 42:213-215.
823 Wetter, D.A., and M.D. Davis. 2009. Lupus-like syndrome attributable to anti-tumor necrosis
824 factor alpha therapy in 14 patients during an 8-year period at Mayo Clinic. *Mayo Clin*
825 *Proc* 84:979-984.
826 Yamada, D.H., H. Elsaesser, A. Lux, J.M. Timmerman, S.L. Morrison, J.C. de la Torre, F.
827 Nimmerjahn, and D.G. Brooks. 2015. Suppression of Fcgamma-receptor-mediated
828 antibody effector function during persistent viral infection. *Immunity* 42:379-390.
829 Zubler, R.H., U. Nydegger, L.H. Perrin, K. Fehr, J. McCormick, P.H. Lambert, and P.A.
830 Miescher. 1976. Circulating and intra-articular immune complexes in patients with
831 rheumatoid arthritis. Correlation of 125I-Clq binding activity with clinical and biological
832 features of the disease. *J Clin Invest* 57:1308-1319.

833

834

835 **Supplemental Data**

836

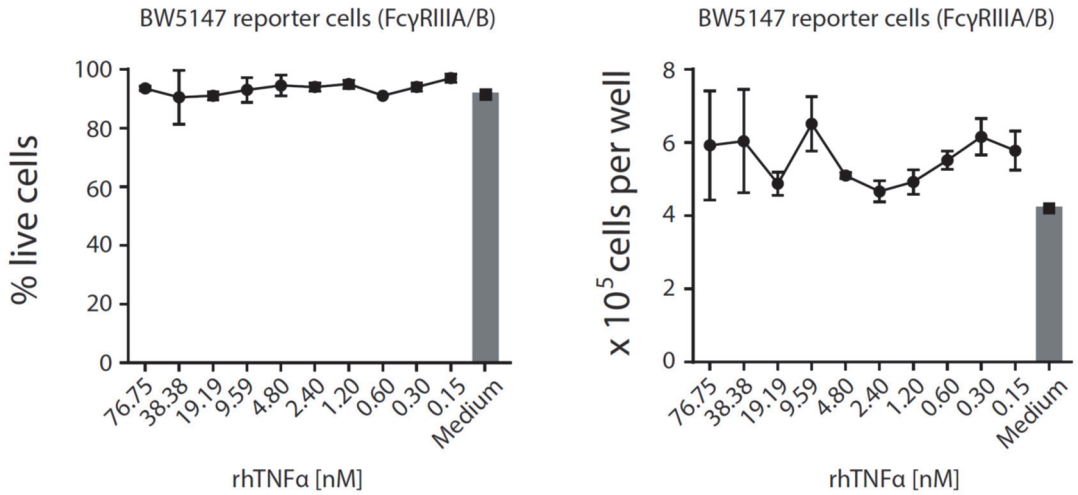

837

838 **Fig. S1. rhTNFα is not toxic to mouse lymphocyte BW5147 cells even at high**
839 **concentrations**. Cell count and percentage of live cells were unaltered over a 16 h time frame
840 of reporter cell culture in the presence of indicated rhTNFα concentrations and comparable to
841 regular growth in complete medium. Experiments were conducted in 3 replicates. Error bars =
842 SD.
843
844

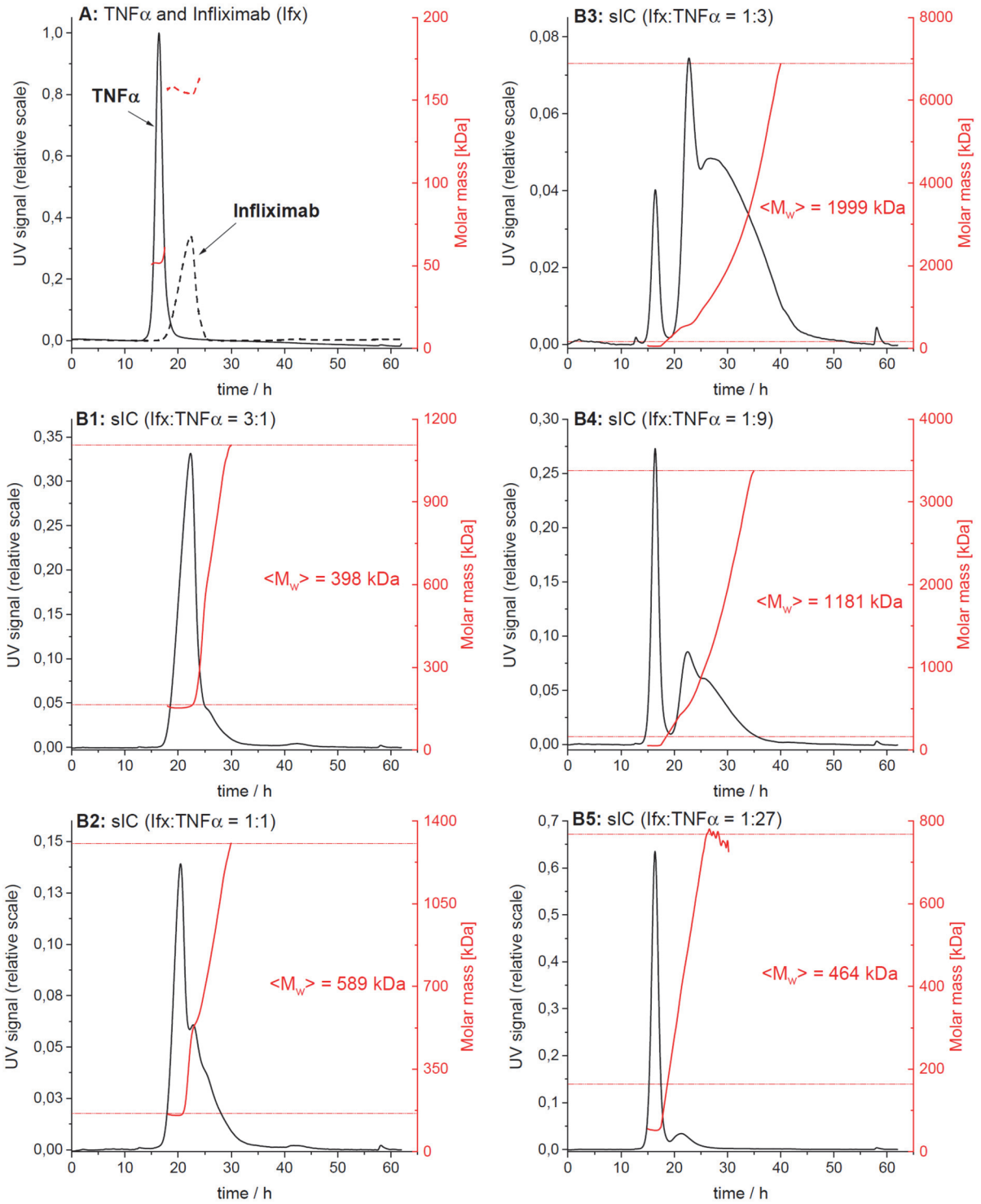

Fig. S2. AF4 elution profiles of Ifx/TNFα-immune complexes.
The elution profiles from one of three independent runs are shown. Protein concentration in the eluate is shown in black (UV signal at λ = 280 nm, normalized to the highest UV signal found in this experiment), molar masses determined by MALS for a given retention time in red. Horizontal red lines indicate the range of molar masses used to calculate the mass-weighted mean of molar masses $<M_w>$. A) Overlay of the elution profiles obtained for TNFα and Ifx, respectively; B1 to B5) Elution profiles for sICs formed after incubation of TNFα and Ifx at different molar ratios.

Sample	Range of assigned molar masses [kDa]			Mass-weighted mean of assigned molar masses [kDa]			
	Run 1	Run 2	Run 3	Run 1	Run 2	Run 3	Mean ± SD
Infliximab, IFX	158 – 182	153 – 164	159 – 193	162	156	163	160 ± 4
TNF -alpha	52 – 55	51 – 61	52 – 62	52	52	52	52 ± 0
Immune complexes							
IFX/TNF 3:1	182 – $1.16 \cdot 10^3$	164 – $1.11 \cdot 10^3$	193 – $1.10 \cdot 10^3$	409	398	518	442 ± 66
IFX/TNF 1:1	182 – $2.06 \cdot 10^3$	164 – $1.31 \cdot 10^3$	193 – $1.42 \cdot 10^3$	801	589	681	690 ± 106
IFX/TNF 1:3	182 – $5.05 \cdot 10^3$	164 – $6.89 \cdot 10^3$	193 – $10.8 \cdot 10^3$	$1.77 \cdot 10^3$	$2.00 \cdot 10^3$	$2.61 \cdot 10^3$	$2.13 \cdot 10^3 \pm 435$
IFX/TNF 1:9	182 – $5.36 \cdot 10^3$	164 – $3.38 \cdot 10^3$	193 – $3.51 \cdot 10^3$	$1.66 \cdot 10^3$	$1.18 \cdot 10^3$	$1.17 \cdot 10^3$	$1.34 \cdot 10^3 \pm 279$
IFX/TNF 1:27	182 – $1.68 \cdot 10^3$	164 – 768	193 – $1.01 \cdot 10^3$	689	464	521	558 ± 117

Table S1. Analysis of the molar mass distribution of ICs from AF4 data.
For a given elution time, the AF4 profiles provide the concentration (UV) at which a given molar mass (MALS) of a protein is present in the sample. The molar mass distribution of Ifx, TNFα and their immune complexes (sICs) was obtained by plotting the cumulative frequency as a function of molar mass. For a selected range of molar masses, a mass-weighted mean value ($<M_w>$) was calculated. All detected molar masses were selected in the case of Ifx and TNFα whereas only molar masses larger than the maximal molar mass found for Ifx were assigned to sICs. The table shows the range of assigned molar masses and the calculated $<M_w>$ for each AF4 run (n = 3).